mei-P22 Encodes a Chromosome-Associated Protein Required for the Initiation of Meiotic Recombination in *Drosophila melanogaster*

Hao Liu,* Janet K. Jang,* Naohiro Kato† and Kim S. McKim*,[1]

**Waksman Institute and Department of Genetics, Rutgers, State University of New Jersey, Piscataway, New Jersey 08854-8020 and* †*Center for Agriculture and the Environment, Rutgers, State University of New Jersey, New Brunswick, New Jersey 08901-8520*

Manuscript received March 7, 2002
Accepted for publication June 17, 2002

ABSTRACT

Double-strand breaks (DSB) initiate meiotic recombination in a variety of organisms. Here we present genetic evidence that the *mei-P22* gene is required for the induction of DSBs during meiotic prophase in Drosophila females. Strong *mei-P22* mutations eliminate meiotic crossing over and suppress the sterility of DSB repair-defective mutants. Interestingly, crossing over in *mei-P22* mutants can be restored to almost 50% of wild-type by X irradiation. In addition, an antibody-based assay was used to demonstrate that DSBs are not formed in *mei-P22* mutants. This array of phenotypes is identical to that of *mei-W68* mutants; *mei-W68* encodes the Drosophila Spo11 homolog that is proposed to be an enzyme required for DSB formation. Consistent with a direct role in DSB formation, *mei-P22* encodes a basic 35.7-kD protein, which, when examined by immunofluorescence, localizes to foci on meiotic chromosomes. MEI-P22 foci appear transiently in early meiotic prophase, which is when meiotic recombination is believed to initiate. By using an antibody to C(3)G as a marker for synaptonemal complex (SC) formation, we observed that SC is present before MEI-P22 associates with the chromosomes, thus providing direct evidence that the development of SC precedes the initiation of meiotic recombination. Similarly, we found that MEI-P22 foci did not appear in a *c(3)G* mutant in which SC does not form, suggesting that DSB formation is dependent on SC formation in Drosophila. We propose that MEI-P22 interacts with meiosis-specific chromosome proteins to facilitate DSB creation by MEI-W68.

MEIOTIC crossovers mature into chiasmata and thereby direct the segregation of homologs at the first meiotic division. It is now commonly accepted that, in many organisms, meiotic recombination is initiated with a double-strand break (DSB), which is then repaired by using the homolog as a template. This process results in either a noncrossover (simple gene conversion) or a crossover (Szostak *et al.* 1983; Lichten 2001). In support of this model, DSBs (reviewed in Goldman and Lichten 1996) and double Holliday junctions (Schwacha and Kleckner 1995) have been detected during meiotic prophase in *Saccharomyces cerevisiae*. While it is not known how DSB sites are chosen, several genetic and epigenetic factors are known to have important roles. For example, at least 10 known gene products are required for DSB formation in *S. cerevisiae* meiosis, and 7 of these are presumed to be meiosis specific (reviewed in Roeder 1997). Some of these proteins could have a role in choosing the DSB site, but one of these proteins, Spo11, is believed to be the enzyme that generates the DSB break. After the DSB has been made, a combination of meiosis-specific and general DSB repair proteins are required for the production of crossovers or gene conversions.

[1]*Corresponding author:* Waksman Institute, Rutgers University, 190 Frelinghuysen Rd., Piscataway, NJ 08854.
E-mail: mckim@rci.rutgers.edu

Few homologs of these DSB-inducing genes have been identified in higher eukaryotes. The significant exception to this observation is Spo11, for which homologs have been identified in several species. Strong mutations in the Drosophila Spo11 homolog, *mei-W68*, eliminate all meiotic recombination, both simple gene conversion and crossing over, from which it has been inferred that the wild-type allele is responsible for making meiosis-specific DSBs (McKim *et al.* 1998). In yeast and mice, DSBs are needed not only for meiotic recombination but also for formation of the synaptonemal complex (SC), a proteinaceous structure that forms between aligned homologs in meiotic prophase (reviewed in Roeder 1997; Lichten 2001). In Drosophila and *Caenorhabditis elegans*, however, SC formation is normal in strong mutants of their Spo11 homologs, implying that in some organisms meiotic recombination is not required for synapsis (Dernburg *et al.* 1998; McKim *et al.* 1998). Further studies and direct observations of DSB formation in higher eukaryotes have technical limitations due to the rarity of DSBs at any given site. Therefore, experiments to determine the time course of key events in a wild-type meiosis such as SC formation, in DSB formation, and in DSB repair have not been possible.

mei-P22 mutants have an identical phenotype to *mei-W68* in that they eliminate meiotic recombination but form normal SC (McKim *et al.* 1998). Here we present genetic evidence that *mei-P22* is required for the initiation of DSBs. Consistent with this function, we have found

that MEI-P22 localizes to foci on meiotic chromosomes, suggesting that MEI-P22 may have a close relationship with DSB formation. Observing the expression pattern of MEI-P22 provides an opportunity to study the regulation of DSB formation in a higher eukaryote. We have found that the binding of MEI-P22 to chromosomes is restricted to a brief period of meiotic prophase and occurs after SC formation. In support of the conclusion that DSB formation is dependent on SC formation, we have found that MEI-P22 localization requires the SC component C(3)G.

MATERIALS AND METHODS

Genetic techniques: All fly crosses to measure X chromosome nondisjunction or crossing over were raised at 25°. The original *mei-P22* mutation, *mei-P22^{1}*, was recovered in a screen for meiotic mutants caused by insertion of a w^+ *P* element (*P{lacW}*; Sekelsky *et al.* 1999). X chromosome nondisjunction was assayed by crossing females to *C(1;Y)1, v f B/0; C(4)RM, ey^{R} ci* males. From this cross, progeny resulting from normal X chromosome disjunction were *B*/+ females and wild-type males. Nondisjunction of the X chromosome resulted in Bar males and wild-type females. Crossing over on the second chromosome was assayed by generating females homozygous for a *mei-P22* mutant and heterozygous for an *al dp b pr cn* chromosome. Crossing over on the third chromosome was assayed by recombining a *mei-P22* mutation onto a *th st cu e ca* chromosome and then backcrossing to make the *mei-P22* mutation homozygous. To assay for radiation-induced crossing over, 2- to 5-day-old virgin females of the genotype *mei-P22^{103}/ mei-P22^{103} th st cu e ca* were exposed to 4000 rad of X rays at a dose of 114 rad/min.

Screen for new *mei-P22* alleles: Males were fed 25 mM ethyl methanesulfonate in 1% sucrose for 24 hr and then transferred to yeasted bottles for 1 day to recover. The cross was conducted as follows:

P_0: *y/y$^+$Y; +/+ ♂ × y w/y w; Dr/TM3* ♀
F_1: *y w/y$^+$Y; +*/Dr or TM3* ♂ × *y w/y w; mei-P22^{1}/TM3*♀
F_2: *y w/y$^+$Y; any thirds* ♂ × *y w/y w; +*/ mei-P22^{1}* ♀

The F_2 cross was brothers to sisters to avoid the requirement for virgins. Normal progeny from this cross were yellow females and wild-type males, whereas the presence of a mutant on the +* chromosome was indicated by yellow males and wild-type females. If these were observed, the cross was set up again for confirmation and a stock made by crossing the white-eyed males and females (*y w/y+Y; +*/TM3* ♂ × *y w/y w; +*/TM3*♀). We could select against the *mei-P22^{1}* chromosome because it is associated with a *P*-element insertion carrying the mini-*white* marker gene.

Molecular analysis of *mei-P22* expression and mutations: Genomic sequences flanking the *P*-element insertion site in *mei-P22^{1}* were isolated and sequenced. An *Eco*RI fragment containing ~1.3 kb of DNA flanking the 3′ end of the *P{lacW}* insertion was isolated by plasmid rescue (Ashburner 1989). The *P*-element was inserted between two open reading frames (ORFs) and could have affected either or both transcripts. The nondisjunction phenotype was rescued by constructs that contained only one of the ORFs. Using the rescue fragment as a probe to screen a Drosophila λ-DASHII genomic library (Finelli *et al.* 1994), we identified three overlapping clones encompassing the *mei-P22* locus. Subclones from one of these were sequenced (GenBank accession no. AF199369). Our sequence differs from that of the genome project by 13 amino acids, perhaps because of different backgrounds (Myers *et al.* 2000 and Figure 3). For *in situ* hybridization, digoxygenin-labeled RNA probes were made from a linearized *mei-P22* clone (pNH4) using the Boehringer Mannheim (Indianapolis) RNA labeling kit and hybridized using a procedure modified from the protocol for embryos (Tautz and Pfeifle 1989).

To sequence our new alleles, some of which were on chromosomes with extraneous lethal mutations, genomic DNA was made from females homozygous for a *mei-P22* allele or that were heterozygous to the original *mei-P22^{1}* allele. PCR was used to amplify the entire *mei-P22* gene. The primers flanked the site of the *P*-element insertion in *mei-P22^{1}*; therefore, in heterozygotes only the DNA from the EMS allele was amplified. Amplified fragments were cloned using the Perfectly Blunt Cloning system (Novagen) and prepared for sequencing by alkaline lysis minipreps and polyethylene glycol precipitation. In some cases, the PCR products were directly sequenced following PCR and isolation from an agarose gel. Sequencing was performed by the University of Medicine and Dentistry of New Jersey sequencing facility and analyzed using the Wisconsin Package Version 9.1 (Genetics Computer Group, Madison, WI). Sequences from different mutant DNAs were compared to identify the nucleotide changes.

Construction and analysis of the *mei-P22* epitope-tag fusion gene: The vector containing the triple hemagglutinin (HA) epitope was constructed by cloning double-stranded oligonucleotides into pBluescript. To make an amino-terminal fusion of *mei-P22* to the epitope tag, the entire coding region, including 1 kb after the stop codon, was amplified by PCR. A *Cla*I site at the amino terminus (introduced in the PCR reaction) and a *Sac*II site were used to clone the fragment into the pBluescript vector containing the epitope tag. The *hsp83* promoter was inserted as a 900-bp *Kpn*I/*Sal*I fragment into the epitope tag/*mei-P22* construct cut with *Kpn*I and *Xho*I. The whole construct was then transferred to the transformation vector pCaSper 4 using the *Kpn*I and *Sac*II sites. We chose to use the *hsp83* promoter because in previous experience it has reliably driven gene expression in the germline. When the *hsp83* promoter was used to drive expression of *mei-218*, we found that every transgenic rescued the *mei-218* mutant phenotype and produced detectable amounts of protein in the germline when examined by immunofluorescence and Western blot (Manheim *et al.* 2002).

With an antibody to the HA tag, we detected approximately equal amounts of MEI-P22^{3XHA} in each of the *hsp83::mei-P22^{3XHA}* transgenics by Western blot of ovarian protein (data not shown). However, in many of these lines, the protein was not detectable in the germline by immunofluorescence and did not rescue the *mei-P22* mutant phenotype. It appeared that certain transgenic lines expressed MEI-P22^{3XHA} in the germline although for unknown reasons it was not visible in the nucleus. An interesting explanation for this finding is based on the observation that the *hsp83::mei-218* transgenic lines differed in the timing of the earliest protein expression. Some lines expressed MEI-218 in early region 2a, whereas in others the protein was not observed until region 2b. Of the transgenics where MEI-P22 was observed, staining was limited to region 2a. Unlike *mei-218*, the timing of MEI-P22 expression appears to be critical for its function: If not present early in the development of the 16-cell cysts, it may be unable to aggregate at potential DSB sites into complexes that are visible by fluorescence. These considerations suggest that the transgenic lines that failed to produce foci expressed MEI-P22 too late in pachytene.

Cytology: For immunolocalization experiments, virgin females were aged for 16 hr at room temperature, dissected, and fixed using the "Buffer A" protocol (Belmont *et al.* 1989). Young females were used to optimize for early germarium stages without the complication of the much larger stage 14 oocytes. All the experiments were performed without heat shock because the basal level of *hsp83* expression is similar to the pattern of *mei-P22* in the germarium. To detect the HA

epitope-tagged MEI-P22, the primary antibody used was either the monoclonal mouse anti-HA 12CA5 (1:20) or the monoclonal rat anti-HA "high affinity" 3F10 (1:100; Roche Biochemicals). The guinea pig anti-C(3)G antibody (Page and Hawley 2001) was used at 1:500, and a combination of two Orb antibodies (4H8 and 6H4; Lantz *et al.* 1994) was used at 1:150. Secondary antibodies were FITC-labeled goat anti-guinea pig (Vector Laboratories, Burlingame, CA) used at 1:300, Cy5-labeled goat anti-mouse (Amersham-Pharmacia) used at 1:40, and Cy3-labeled goat anti-rat (Amersham-Pharmacia or Jackson ImmunoResearch) used at 1:250. Chromosomes were stained with 4′,6-diamidino-2-phenylindole (0.2 μM) for 10 min or Hoechst (0.1 μl/ml of a 10 mg/ml solution) for 5 min. For immunolocalization of DSBs, the anti-phospho-H2AX (Ser139) rabbit polyclonal antibody (Upstate Biotechnology, Lake Placid, NY; Rogakou *et al.* 1999) was used at 1:100 and the secondary Cy3-labeled goat anti-rabbit (Amersham) was used at 1:300.

For BrdU staining, ovaries were incubated with 10 mM BrdU (Sigma, St. Louis) in Grace's insect cell culture medium (Life Technologies) for 1 hr. The ovaries were then fixed as described above and washed 2 × 15 min in PBS + 0.6% Triton-X100 and 2 × 15 min in DnaseI buffer (Life Technologies) and then incubated in 25 units DnaseI (in 0.5 ml DnaseI buffer) at 37° for 30 min. Monoclonal mouse anti-BrdU (Becton-Dickinson, San Jose, CA) was used at 1:20.

Most of the images were collected using a Leica TCS SP2 confocal microcope or a Zeiss Axioplan II imaging microscope equipped with a Cooke Sensicam CCD camera. All images were collected using a ×63 or ×100 objective. For analysis by deconvolution, the images were collected with a DeltaVision restoration microscopy system (Applied Precision) equipped with a Nikon ×60 N.A.1.4 oil immersion objective. The restoration and modeling was performed with softWoRx software (Applied Precision) on an Octane Workstation (Silicon Graphics).

RESULTS

The effect of *mei-P22* on chromosome disjunction and crossing over: Previous studies found that the *mei-P22^{1}* mutation caused a reduction in the frequency of gene conversion, which is evidence that *mei-P22* has a role in initiating meiotic recombination (McKim *et al.* 1998). This mutation was not ideal for further studies because it is not a null allele (see below). We isolated four additional *mei-P22* mutations (materials and methods) and characterized their effects on X chromosome nondisjunction (Table 1) and crossing over (Table 2). Two, *mei-P22^{205}* and *mei-P22^{206}*, were weaker alleles and had relatively low X chromosome nondisjunction. Crossing over in *mei-P22^{206}* homozygotes was decreased to ~50% of wild type in the *cu-e* and *e-ca* regions. In the *st-cu* region, however, crossing over was increased to 156% of wild type. The *st-cu* region includes the centromere and in wild type exhibits crossover suppression relative to the genome average. Therefore, these results show that the crossover reductions in *mei-P22^{206}* were accompanied by a change in the distribution of residual events along the chromosome. In Drosophila, many, although not all, recombination-defective mutants also change the distribution of crossing over relative to wild type ("precondition mutants"; Baker and Hall 1976).

TABLE 1

Transgenic rescue of X chromosome nondisjunction in *mei-P22* mutants

Genotype	ND (%)	Total progeny
mei-P22^{1}/ +	0.4	1414
mei-P22^{1}/mei-P22^{1}	38.5	577
mei-P22^{103}/mei-P22^{103}	37.4	1182
mei-P22^{205}/mei-P22^{205}	15.8	501
mei-P22^{206}/mei-P22^{206}	3.2	4374
mei-P22^{N1}/mei-P22^{N1}	41.6	1267
P{hsp83::mei-P22^{3XHA}} 9/+, mei-P22^{N1}	2.9	621
P{hsp83::mei-P22^{3XHA}} X1/+; mei-P22^{N1}	8.3	555
P{hsp83::mei-P22^{3XHA}} 4/+; mei-P22^{N1}	5.0	947
P{hsp83::mei-P22^{3XHA}} 2/+; mei- P22^{N1}	36.4	638

ND, nondisjunction.

The other two mutations, *mei-P22^{103}* and *mei-P22^{N1}*, caused higher levels of X chromosome nondisjunction and drastically reduced the frequency of crossing over. *mei-P22^{103}* may be a null allele because it reduced crossing over to extremely low levels (0.3% of wild type) similar to the *mei-W68* mutant phenotype. *mei-P22^{N1}* had a low level of crossing over on the third chromosome (13% of wild type), suggesting that it reduced but did not eliminate the initiation of recombination. Crossing over was more severely affected on the second chromosome in *mei-P22^{N1}* females (4.2% of wild type), suggesting that in this mutant the recombination frequency was sensitive to the chromosome or genetic background. The *mei-P22^{N1}* second chromosome crossover frequency was similar to our observations with the original allele *mei-P22^{1}*, suggesting that this mutation is also not a null allele.

***mei-P22* mutants lack DSBs:** The initial step in meiotic recombination is the formation of DSBs. To examine whether *mei-P22* is required before or after establishment of DSBs, we performed two experiments. The first experiment was to determine if an exogenous source of DSBs, X rays, could rescue a strong *mei-P22* mutant phenotype. The second experiment was to determine if a *mei-P22* mutation could suppress the phenotype of a mutant defective in the repair of DSBs.

Previous experiments have shown that X-irradiation partially rescues the meiotic recombination defect in mutants unable to generate DSBs, including *spo11* homolog mutants of *S. cerevisiae* (Thorne and Byers 1993), *C. cinereus* (Celerin *et al.* 2000), *C. elegans* (Dernburg *et al.* 1998), and Drosophila (R. Bhagat and K. McKim, unpublished results). Conversely, irradiation has no effect on *mei-218* mutants that act after DSB formation or in *c(3)G* mutants (Roberts 1969; R. Bhagat and K. McKim, unpublished results). We exposed *mei-P22^{103}* mutant females to 4000 rad of X-irradiation, crossed them with males to score either crossing over or X chromosome nondisjunction, and then transferred

TABLE 2

Third chromosome crossing over (cM) in *mei-P22* mutants

Genotype	Third chromosome genetic interval (cM)			Total map (% of wild type)[b]	Total progeny
	st cu[a]	*cu e*	*e ca*		
+/+	3.2	17.3	30.4	50.9	618
mei-P22^{206}/*mei-P22*^{206}	5.0	6.7	17.6	29.3 (57.6)	1511
mei-P22^{N1}/*mei-P22*^{N1}	3.5	1.2	1.6	6.3 (12.4)	487
mei-P22^{103}/*mei-P22*^{103}	0.06	0.06	0.06	0.2 (0.3)	1703
mei-P22^{103}/*mei-P22*^{103} *(X-ray)*[c]	6.2	7.4	7.6	21.2 (41.6)	434
P{mei-P22^{3XHA}*}9/+; mei-P22*^{103}	1.0	33.2	23.1	57.3 (112.6)	1309

Genotype	Second chromosome genetic interval				Total map (% of wild type)[b]	Total progeny
	al-dp	*dp-b*	*b-pr*	*pr-cn*[a]		
+/+	13.3	18.1	4.0	0.7	36.1	955
mei-P22^{N1}/*mei-P22*^{N1}	0.5	0.5	0.5	0	1.5 (4.2)	937
mei-P22^{1}/*mei-P22*^{1}	0.2	0.8	0.2	0.3	1.5 (4.2)	2590

For the third chromosome, *th st cu e ca*/+++++ females were crossed to *ru h th st cu e Pr ca/TM6B* males. For the second chromosome, *al dp b pr cn*/+++++ females were crossed to *al dp b pr cn* males.

[a] This interval includes the centromeric region.

[b] The map distance between *th* and *ca* or *al* and *cn*. The percentage of the wild-type control is in parentheses.

[c] Data are from the 4- to 6-day brood, the most sensitive to X-irradiation (see text). In this experiment, and in the others in this table, approximately equal numbers of the reciprocal crossover progeny were recovered.

them to new vials every 3 days. Crossing over was induced by as much as 120-fold compared to unirradiated controls, almost half of wild-type levels (Table 2 and Figure 1), demonstrating that exogenously induced DSBs could compensate for the *mei-P22* defect. Nondisjunction was also decreased, as was expected if the induction of crossing over resulted in chiasmata that could direct the segregation of homologous chromosomes. The most significant increases in crossing over and decreases in X chromosome nondisjunction were observed in the offspring derived from oocytes fertilized 4–6 days after radiation treatment. In these offspring, for example, X chromosome nondisjunction was reduced to 7.9% in contrast to 34.6% in unirradiated mutant females. These oocytes were in pachytene when their mothers were exposed to X rays (King 1970; Spradling *et al.* 1997), suggesting that there is a limited time frame in oogenesis during which DSBs efficiently generate crossovers.

The *st-cu* region of the third chromosome was more sensitive to radiation-induced crossing over than were other regions. In the 4- to 6-day brood, crossing over in the *st-cu* interval occurred at 194% of wild type, whereas in the more distal *cu-ca* region crossing over occurred at 31% of wild type. The *st-cu* region was also significant because crossing over was induced by radiation at relatively high levels through all broods. In contrast, an increased frequency of crossing over in the *cu-e* and *e-ca* regions occurred only in the 4- to 6- and 7- to 9-day broods (data not shown). From the markers used, we cannot determine if these interval-specific effects of the *st-cu* region are a result of heterochromatic crossovers or if X-ray-induced crossovers exhibit the same changes in distribution observed with endogenously induced crossovers in *mei-P22* hypomorphs.

As a second test of the relationship between *mei-P22* function and DSB formation, we constructed a double mutant with *spnB*^{BU}. *spnB* encodes a meiosis-specific Rad51 homolog and is required for meiotic DSB repair. *spnB* mutants are sterile because defects in meiotic DSB repair cause the oocyte to develop abnormally (Ghabrial *et al.* 1998). Mutants that eliminate DSBs, such as *mei-W68*, suppress the oogenesis defects and partially restore fertility to *spnB* (Ghabrial and Schupbach 1999; R. Patel and K. McKim, unpublished results). In females homozygous for both *mei-P22*^{N1} and *spnB*^{BU}, fertility was increased more than threefold compared to those for *spnB*^{BU} alone (Figure 2). While the *spnB*^{BU} mutant females are completely sterile by the time they have been laying eggs for 3 days, the *mei-P22*^{N1} *spnB*^{BU} double mutants continued to produce progeny as they aged. This increase in fertility was similar to that observed with *mei-W68*^{1}*; spnB*^{BU} homozygotes and is consistent with a failure to create DSBs in *mei-P22* mutants. The fact that the fertility in the double mutants was not restored to *mei-P22* (or *mei-W68*) single-mutant levels indicates that *spnB* might have additional roles during oogenesis.

Finally, we employed a cytological assay of DSB cre-

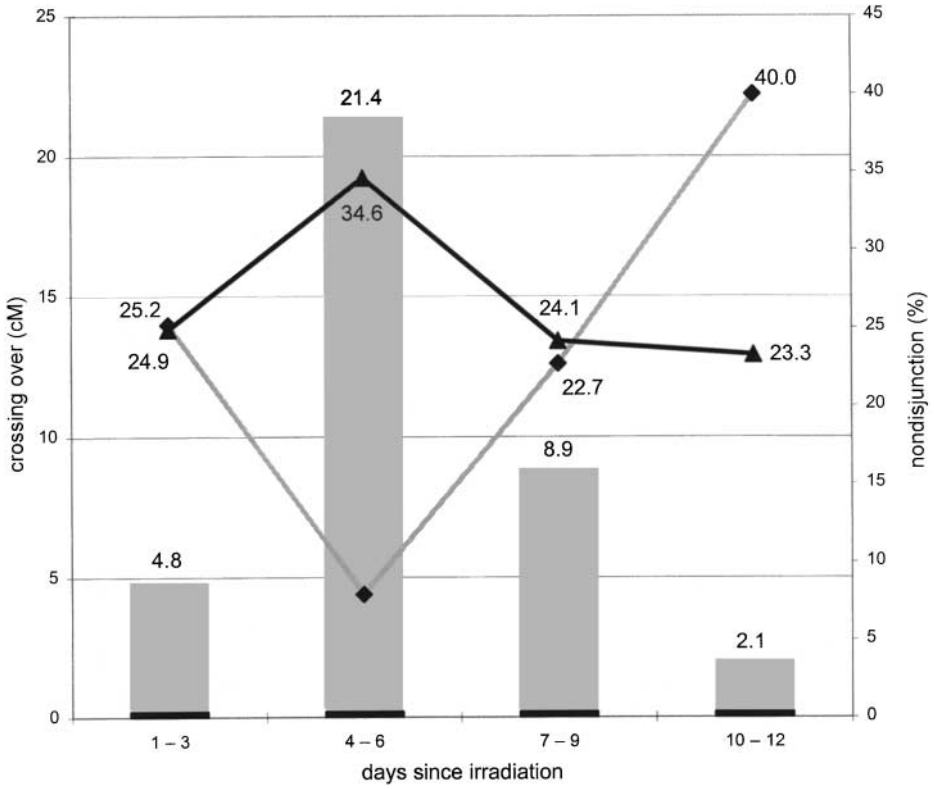

FIGURE 1.—Crossing over is increased and nondisjunction decreased by irradiating *mei-P22*^{103} females. The frequency of crossing over between *st* and *ca* (control distance = 50.9) is shown with shaded (irradiated) or solid (not irradiated) bars. Nondisjunction frequencies are shown with shaded (irradiated) or solid (not irradiated) lines. The high nondisjunction frequency for the irradiated 10- to 12-day brood may not be significant due to a small sample size.

ation by using an antibody to the phosphorylated form of human H2AX (γ-H2AX), which detects a histone modification that occurs at DSBs in meiotic cells of male mice (MAHADEVAIAH *et al.* 2001). We have shown that this antibody detects DSB-dependent foci during meiotic prophase of Drosophila females (D. SHERIZEN, J. K. JANG and K. MCKIM, unpublished results). In *mei-P22*^{N1} and *mei-P22*^{103} mutants, these foci were not observed (data not shown). This result is most striking, however, when a *spnB* double mutant is examined because the foci of γ-H2AX staining persist longer in DSB repair-defective mutants than in wild type (D. SHERIZEN and K. MCKIM, unpublished results). An example of this is shown in Figure 2B; all oocytes from *spnB*^{BU} females accumulate γ-H2AX foci late in meiotic prophase. In a *mei-P22*^{N1} *spnB*^{BU} double mutant, however, these foci were not observed. It is likely that γ-H2AX foci are absent in the double mutant because DSBs are not created in a *mei-P22* mutant.

***mei-P22* encodes a small, novel, basic protein:** Genomic sequences flanking the *P*-element insertion site in *mei-P22*^{1} were used to clone the gene (MATERIALS AND METHODS). The assignment of the *mei-P22* coding region was confirmed by rescuing mutants with transgenes and the sequencing of mutations. The original *P*-element mutation inserted 52 bp upstream of the ATG. For each of the *mei-P22* EMS alleles, we identified a single nucleotide sequence change within the coding region (Figure 3). The two severe EMS alleles *mei-P22*^{N1} and *mei-P22*^{103} were found to be stop codons while the hypomorphs *mei-P22*^{205} and *mei-P22*^{206} were missense mutations. Surprisingly, some genetic tests showed *mei-P22*^{N1} to be a weaker allele than *mei-P22*^{103} (*e.g.*, Table 2). Hypomorphic alleles that are stop codons have been observed in the meiotic recombination genes *mei-9* and *mei-217* (MANHEIM *et al.* 2002; J. SEKELSKY, personal communication). In this case, it is possible that in some genetic backgrounds there may be a low frequency of translational readthrough of the *mei-P22*^{N1} stop codon. Genomic sequence analysis and RT-PCR (data not shown) showed that *mei-P22* encodes a 954-bp ORF with no introns. MEI-P22 is predicted to be 318 amino acids with a potential bipartite nuclear localization sequence (NLS) between amino acids 145 and 162, has a predicted isoelectric point of 10.23, and has no homologs in the sequence databases (Figure 3).

We used the *hsp83* promoter to express the transgene because its expression pattern in the germarium is similar to that of *mei-P22* (see below), and we experienced difficulties achieving transgenic rescue of the mutant phenotype with the endogenous promoter, presumably due to position effects. Fused to the 5′ end of the *mei-P22* coding region was an epitope tag encoding three hemagglutinin (3XHA) peptide sequences to facilitate immunolocalization of the protein (see below). Several *hsp83::mei-P22*^{3XHA} transgenic lines that rescued the *mei-P22* mutant phenotype were isolated as well as some that did not (Table 1 and MATERIALS AND METHODS).

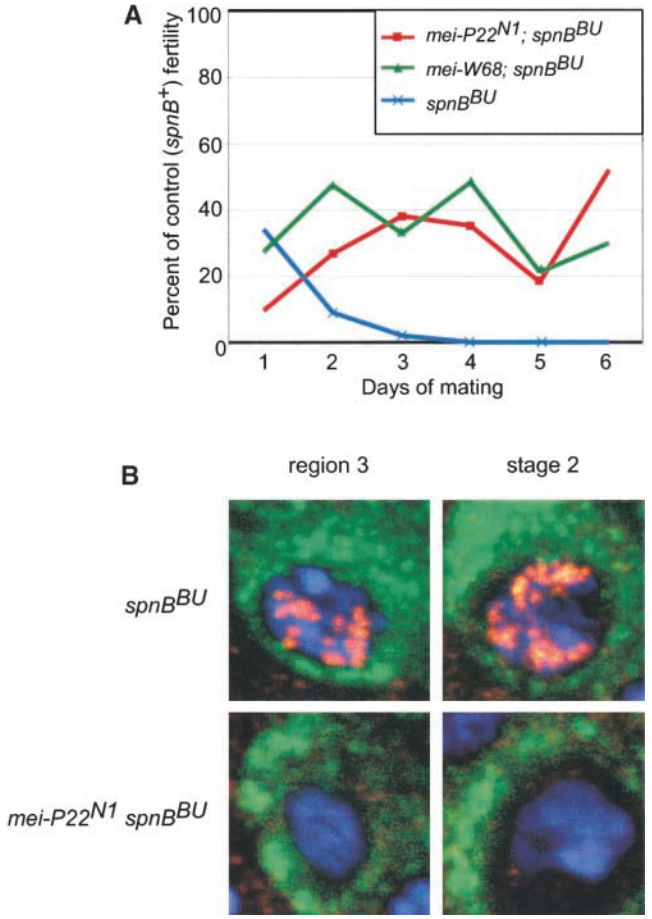

FIGURE 2.—*mei-P22* is epistatic to *spnB* mutants. (A) $spnB^{BU}$ mutants are sterile after the first 2–3 days of mating (blue). This effect is suppressed by mutations that reduce DSBs such as $mei\text{-}W68^{I}$ and $mei\text{-}P22^{N1}$. (B) Unrepaired DSBs are present in a $spnB^{BU}$ mutant but not a $mei\text{-}P22^{N1}$ $spnB^{BU}$ double mutant. In each image the oocyte was recognized due to the enrichment of the ORB protein in the cytoplasm (green). Region 3 and stage 2 oocytes are in a relatively late stage of meiotic prophase (see also Figure 4). In wild type the γ-H2AX foci are usually absent because the DSBs have been repaired. In a *spnB* mutant, however, the γ-H2AX antibody stains numerous foci because the DSBs are not repaired (D. SHERIZEN and K. MCKIM, unpublished results). In the $mei\text{-}P22^{N1}$ $spnB^{BU}$ double mutant no foci were visible, suggesting that the DSBs were never formed.

Analysis of *mei-P22* expression: overview of Drosophila oogenesis: Our analysis of *mei-P22* RNA and protein expression was performed using whole mounted ovaries. Not only did this approach maintain the three-dimensional structure of the meiotic cells, but it also allowed us to determine the time course of MEI-P22 expression since cells in the ovary are arranged in order of developmental age. An overview of Drosophila oocyte development is described below, and a schematic of the germarium and summary of our results are shown in Figure 4A.

Drosophila females have two ovaries, each composed of 10–15 ovarioles containing chains of developing oocytes. At the anterior end of each ovariole is the germarium, where four rounds of incomplete mitotic divisions produce a 16-cell cyst with intercellular junctions termed ring canals. Although each cyst will eventually contain just one oocyte, several cells enter meiosis. Specifically, the SC first develops in the two cells with four ring canals (the pro-oocytes) and later SC develops to variable extents in the other cells with fewer ring canals. Eventually, all cells but the oocyte exit the meiotic program and SC is maintained in only one cell, the oocyte (CARPENTER 1975a, 1979).

The cysts move down the germarium as they mature but their absolute position does not equate to a specific stage in meiotic prophase (CARPENTER 1975a). More significantly, the cysts are usually arrayed in order of developmental age such that a cyst in a posterior position is usually at a later stage of meiotic prophase than that of a cyst in a more anterior position. There can be exceptions to this arrangement, but relative cyst position is a useful tool to identify and compare oocytes in different stages of meiosis (Figure 4A). The germarium is divided into four regions on the basis of the morphology of the 16-cell cysts, which we distinguished using an antibody to the ORB protein (LANTZ *et al.* 1994). ORB is a cytoplasmic protein that first appears in early region 2a and becomes enriched in the oocyte by region 2b. In region 2a of the germarium, meiotic prophase begins and recombination is initiated (CARPENTER 1979).

***mei-P22* RNA is expressed in the germarium:** We were able to detect *mei-P22* mRNA in the Drosophila ovary using *in situ* hybridization with an antisense RNA probe. *mei-P22* RNA was specifically observed in the postmitotic region of the germarium, in regions 2 and 3 where meiotic prophase occurs (Figure 4B). No staining was observed in later stages of the vitellarium. In contrast, we were unable to detect the transcript by Northern blot of ovary total RNA or by screening two ovarian cDNA libraries, suggesting that the transcript is rare (data not shown).

MEI-P22 protein is detected during early meiotic prophase: To gain further insights into the function of *mei-P22* and its relationship to DSB formation, we examined the localization of the protein. Since two attempts at raising antibodies to the endogenous protein failed, we used the rescuing transgenes (described above) containing the *mei-P22* coding region fused at the amino terminus to three copies of the HA epitope tag. For most immunolocalization experiments we used the transformant line $P\{hsp83::mei\text{-}P22^{3XHA}\}9$ because it provided the best rescue of the *mei-P22* mutant defects in disjunction (Table 1) and crossing over (Table 2). The efficient rescue was possible because the *hsp83* promoter drives expression without heat shock throughout regions 2 and 3 of the germarium (DING *et al.* 1993; MANHEIM *et al.* 2002).

When Drosophila ovaries carrying the *P{hsp83::mei-*

```
  1  MDRATVVPSP ASTYCSFMGG SQHSPLRRSQ RLIDKENRDL QKIPPKSLSP

 51  QLFGNTEDDY SELLLQQGKV VHLKPAAKLV PVRSSDNLVH LGSRDKVVPL

101  KTSNRIVHLK PSYKIIHLKS LDEVEKTVKK KNNTQKEVHQ RNSQRRSIQC
             stop(N1)                                      ▼
151  TPKKRGRKPK QPAKKLQSRI STDQLGNTPS PSKLPAKYPA HFVHQLPPAA

201  PAMQLSDLSL TPDEIQTPER RGEIVNKSPS DLDSDVSLNI SLSDSIGEIF
                   I(206)            stop(103)   A(205)
251  GTKDISSILT MQRPRQYILL EEHLPTLATM LNVDLERLRC VLDITQGLSH

301  EQILRFPIKH EEDELEVS
```

FIGURE 3.—Sequence of MEI-P22 including the changes in the EMS mutants. The sequence shown corresponds to our sequence from the λ-DASHII library. In the published genome sequence, there is an insertion (arrowhead) encoding 13 amino acids (EDSSCAT RRRSLS; MYERS *et al.* 2000). The positions of EMS-induced mutations are shown in boldface type, the predicted BP-NLS is underlined, and the region predicted to form an α-helix is shown in italic.

P22^{3XHA}*} 9* transgene were stained with an anti-HA antibody, MEI-P22 fusion protein was detected in region 2a of the germarium (Figures 4 and 5). This staining pattern was observed whether the transgene was in a wild-type or *mei-P22* mutant background. On the basis of a comparison to ORB staining, MEI-P22 staining was restricted to region 2a (*i.e.*, early pachytene) and usually disappeared by the end of region 2a (Table 3), suggesting that relative to other events in the oocyte, MEI-P22 staining is short lived. In addition, MEI-P22 staining appeared as numerous foci, and because it always overlapped with the DNA stain, it appears to be a nuclear protein (Figure 5A). Similar patterns were observed with other transgenic lines that rescued the *mei-P22* mutant phenotype, such as *P{hsp83::mei-P22*^{3XHA}*} 4* and *P{hsp83::mei-P22*^{3XHA}*} X1*. No staining was observed in transgenics that failed to rescue the mutant phenotype such as *P{hsp83::mei-P22*^{3XHA}*} 2* (data not shown).

Evidence for post-transcriptional regulation of *mei-P22*: The MEI-P22 expression pattern may be the result of post-transcriptional regulation. The mRNAs of *mei-P22* (Figure 4) and *hsp83* (DING *et al.* 1993) are expressed throughout regions 2 and 3 of the germarium. Furthermore, when the *hsp83* promoter was used to drive expression of *mei-218*, protein was observed in regions 2 and 3 of the germarium (MANHEIM *et al.* 2002). Thus, we suspect that the mRNA from the *P{hsp83::mei-P22*^{3XHA}*} 9* transgene is expressed throughout regions 2 and 3. In contrast, MEI-P22 was detected in a more restricted pattern and was never observed in region 3 cells.

In addition to expression in the germarium, using the *hsp83* promoter resulted in expression of *mei-P22* protein in a subset of the somatic follicle cells (Figure 5C). Because the follicle cells are asynchronously dividing, this result suggests that MEI-P22 levels or nuclear entry are regulated at a post-transcriptional level by the cell cycle. Therefore, the mechanism that causes MEI-P22 to be present for only a limited portion of meiotic prophase could also be functioning in mitotic cells. In contrast to this similarity in regulation, the pattern of nuclear staining in the meiotic (germline) and mitotic (follicle) cells differed in appearance. Unlike the discrete foci observed in the germline meiotic cells, mitotic cell nuclear localization was uniformly spread along the chromosomes. This difference suggests that there must be meiosis-specific factors that restrict the binding of MEI-P22 to a small number of chromosomal sites during meiotic prophase.

MEI-P22 appears after SC formation begins: To accurately relate MEI-P22 localization to meiotic events in the oocyte, we compared the localization of MEI-P22 to the development of the SC. To detect the presence of the SC, we used an antibody to the *c(3)G* protein, which is proposed to be a component of the transverse elements (PAGE and HAWLEY 2001). Prior to ORB localization, SC formation is the earliest indicator of the oocyte. C(3)G antibody staining was observed in at least the two pro-oocytes in each region 2a cyst. In addition, C(3)G stained transiently in additional cells of some region 2a cysts but was usually limited to the oocyte by region 3 (Figure 4).

In ~50% of the germaria, there was one early region 2a cyst with C(3)G staining but no MEI-P22 foci or ORB staining (Figure 4C). These cysts are probably a normal stage in ovary development but were not observed in all germaria because they persist for a short period of time. These cells also stained lighter for C(3)G, suggesting that they are at the zygotene-pachytene transition. As noted by CARPENTER (1975a), zygotene is a relatively brief stage of prophase in Drosophila. In the remaining germaria, the earliest MEI-P22 was observed simultaneously with the appearance of ORB and C(3)G staining (Figures 4D and 5A). MEI-P22 was never observed in a cyst that did not have C(3)G staining in the oocyte. On the basis of these data, we conclude that SC forms first and is rapidly followed by MEI-P22 accumulation.

There is probably an indirect relationship between C(3)G and MEI-P22. That is, although the MEI-P22 localization occurred after and was dependent on C(3)G, these proteins may not directly interact. Three-dimensional reconstructions of deconvolved image stacks revealed that MEI-P22 usually occupied a space that was separate from SC, although the foci always overlapped the DNA staining (Figure 6). These observations suggest that SC development alters the chromosomes to allow MEI-P22 binding.

MEI-P22 foci transiently associate with pachytene chromosomes: Compared to the other cells in each 16-cell cyst, C(3)G staining is the strongest and forms the most threadlike structures in the two pro-oocytes (Page and Hawley 2001). Abundant MEI-P22 foci were observed in the nuclei of these cells but usually in only two to four cysts per germarium (Table 3). Some pachytene pro-oocytes in late region 2a and all in region 2b had no MEI-P22 staining, however, suggesting that the appearance and disappearance of MEI-P22 foci in the pro-oocytes is rapid. For example, MEI-P22 foci were usually observed in the pro-oocytes at the earliest stages of pachytene, whereas oocytes that appeared to be in later stages of pachytene, such as those in more posterior located cysts of region 2a and 2b, lacked MEI-P22 foci (Figure 4D). The nurse cells in region 2a cysts usually contained MEI-P22 foci as well. These MEI-P22 positive nurse cells often had punctate C(3)G staining, suggesting that they had partially entered the meiotic program. In fact, in late region 2a cysts MEI-P22 foci commonly were still present in the nurse cells even though they had disappeared from the pro-oocytes. Furthermore, the foci were more abundant in some nurse cells than in the pro-oocytes. These observations of the nurse cells suggest that MEI-P22 accumulated for a longer time in those cells where SC did not fully develop (Figure 4D).

While initially surprising, the presence of MEI-P22 in

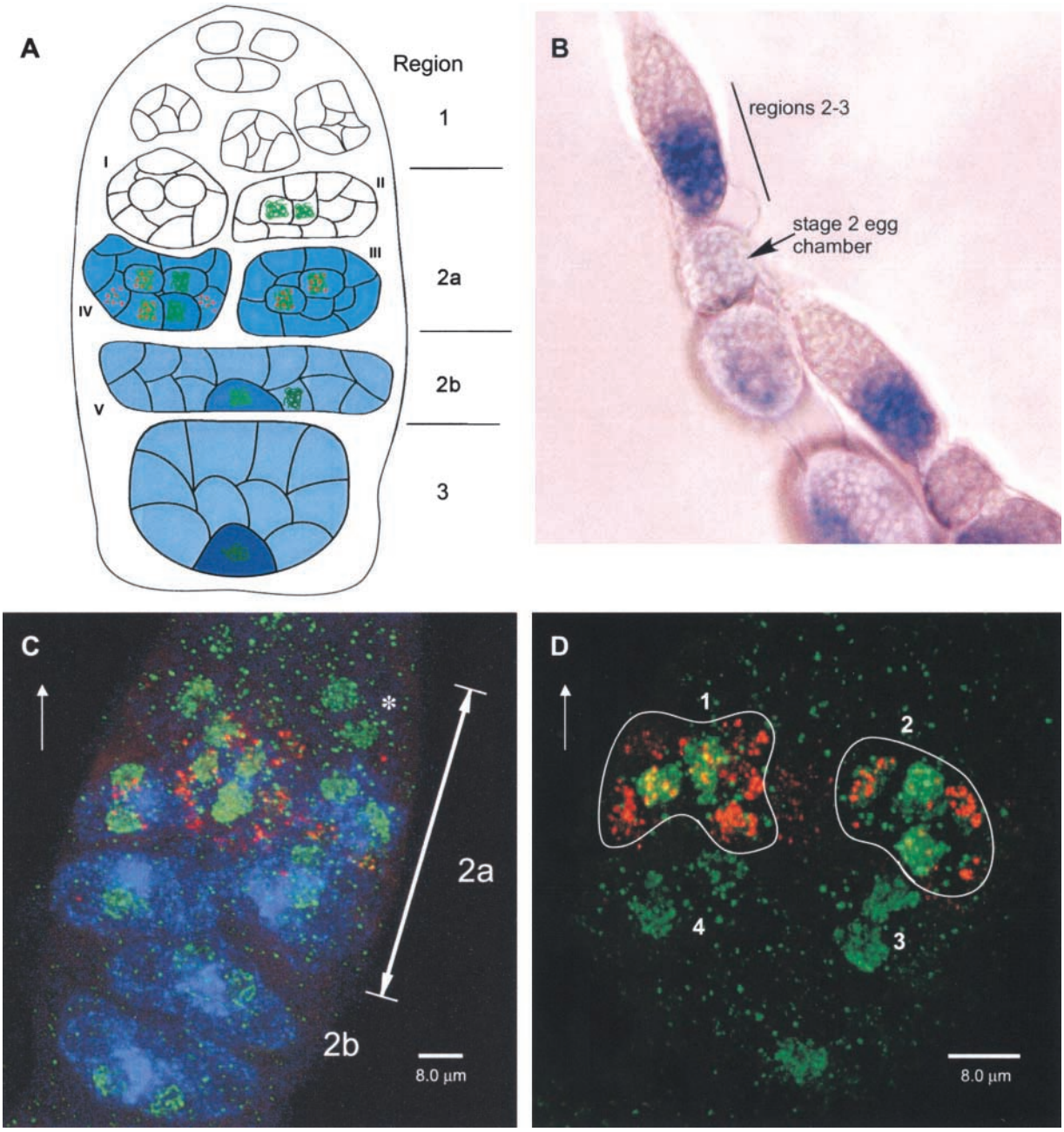

TABLE 3

MEI-P22 staining in different mutant backgrounds

Genetic background	MEI-P22 positive cysts per germarium[a]	Germaria with MEI-P22 in region 2b[b]	MEI-P22 foci per SC containing cell[c]	Total germaria
Wild type	3.8	0	8.7	12
spnB^{BU}	6.8	7	13.6	7
mei-W68^{4572}	6.0	8	10.3	8
c(3)G^{68}	0	—	0	13

ND, not determined.

[a] The average number of cysts per germarium that contained MEI-P22-staining nuclei in nurse cells and/or pro-oocytes. In wild type usually only one cyst had pro-oocyte staining whereas in the mutants most cysts had pro-oocyte staining.

[b] The number of germaria that had MEI-P22 staining in at least one region 2b cyst.

[c] The average number of foci in the two cells in each region 2a cyst with four-ring canals and complete SC formation (pachytene) that also had MEI-P22 foci.

cells fated to become nurse cells can be explained in the context of germline cyst development. While some of the nurse cell staining could be due to abnormally high expression levels from the transgene, there is also good evidence based on the appearance of recombination nodules (Carpenter 1994) and the detection of DSBs with antibodies (D. Sherizen and K. McKim, unpublished results) that the nurse cell progenitors experience double-strand breaks. Given that SC develops in several cells of the 16-cell cyst, but then rapidly degrades, and that *c(3)G* is required for MEI-P22 localization, one possibility is that MEI-P22 accumulates only in regions of the chromosomes where SC previously developed. Cells with punctate C(3)G staining may have persistent MEI-P22 foci because the completion of SC formation (pachytene) and/or DSB repair in the pro-oocytes may hasten the removal of MEI-P22 from the chromosomes. This conclusion is supported by our findings, described below, that delays in DSB repair alter the dynamics of the MEI-P22 foci.

The relationship of MEI-P22 localization to double-strand-break repair: To determine if DSB repair plays a role in removing MEI-P22 from meiotic chromosomes, we stained for foci in mutants where DSBs either do not form or are not correctly repaired. We constructed *hsp83::mei-P22*^{3XHA} *mei-W68*^{4572} females to observe MEI-P22 localization when DSBs do not occur (meiotic recombination is eliminated in a *mei-W68*^{4572} mutant) and *hsp83::mei-P22*^{3XHA} ; *spnB*^{BU} females to observe MEI-P22 when there is a defect in DSB repair (Ghabrial *et al.* 1998). In both types of females, we found that MEI-P22 foci appeared at the normal time in region 2a, but there were two important differences from the wild-type dynamics of the foci. First, in both *mei-W68* and *spnB* mutants, the MEI-P22 foci usually persisted into region 2b cysts (Figure 7). Second, based on double staining

Figure 4.—Expression of *mei-P22* in the germline. (A) Schematic diagram of the Drosophila germarium showing the stages of development, SC formation (green), and MEI-P22 foci dynamics (red). Not all 16 cells in each cyst are shown. In region 1, four rounds of mitotic divisions create the 16-cell cysts. Cytoplasmic ORB staining (blue) is initially equal in all 16 cells and then localizes to the oocyte late in region 2a. The first SC forms in the 2 cells with four intercellular connections or ring canals, the pro-oocytes. Later, more cells form SC, with the 2 three-ring canal cells forming extensive amounts, although distinguishable from the 2 four-ring canal cells by comparatively lighter staining with C(3)G. In region 2b cysts, the cells flatten out. Finally, all cells but the oocyte exit the meiotic program and lose their SC. On the basis of cyst position and ORB, C(3)G, and MEI-P22 staining, we propose four stages of meiotic prophase in region 2a cysts (labeled I–IV). In temporal order they are: (I) cysts with no SC, ORB, or MEI-P22; (II) cysts that stain with C(3)G but lack cytoplasmic ORB and nuclear MEI-P22 staining; (III) cysts with cytoplasmic ORB and MEI-P22 in the nucleus of the 2 cells with C(3)G, the pro-oocytes; (IV) cysts with C(3)G staining in additional cells, such as those with three- or two-ring canals; MEI-P22 persists in these cells and may be absent from the 2 four-ring canal cells; and (V) cysts with SC, which is beginning to be restricted to the oocyte, but in which MEI-P22 is absent. (B) *mei-P22* is expressed during meiosis in the Drosophila ovary. *In situ* hybridization using an antisense RNA probe for the *mei-P22* coding region is shown. The figure is labeled to show how the transcript is enriched in the germarium. Stage 2 cysts are the first stage of the vitellarium. The staining on the edge of some vitellarium cysts is nonspecific. (C) MEI-P22 (red) appears early in the germarium. The anterior of the germarium, and hence the earlier stages of development, is at the top in B–D and is shown by an arrow. In this volume projection of a confocal stack of images, C(3)G (green) appears prior to the earliest appearance of ORB (blue) and MEI-P22 (asterisk). Late region 2a and region 2b cysts have no MEI-P22 foci. (D) Volume projection of confocal images showing MEI-P22 (red) closely associated with C(3)G (green). A white outline shows the approximate shape of four region 2a cysts, two with MEI-P22 staining. The logically inferred developmental order of the cysts is indicated by a number. In cyst 1, MEI-P22 appears in the two nuclei with the strongest C(3)G staining (pro-oocytes) but also in nuclei with weaker staining (nurse cells). In cyst 2, MEI-P22 is present at low levels in the pro-oocytes and is most abundant in cells with punctate C(3)G staining. In later stage cysts (3 and 4) the oocytes still have C(3)G staining but no MEI-P22.

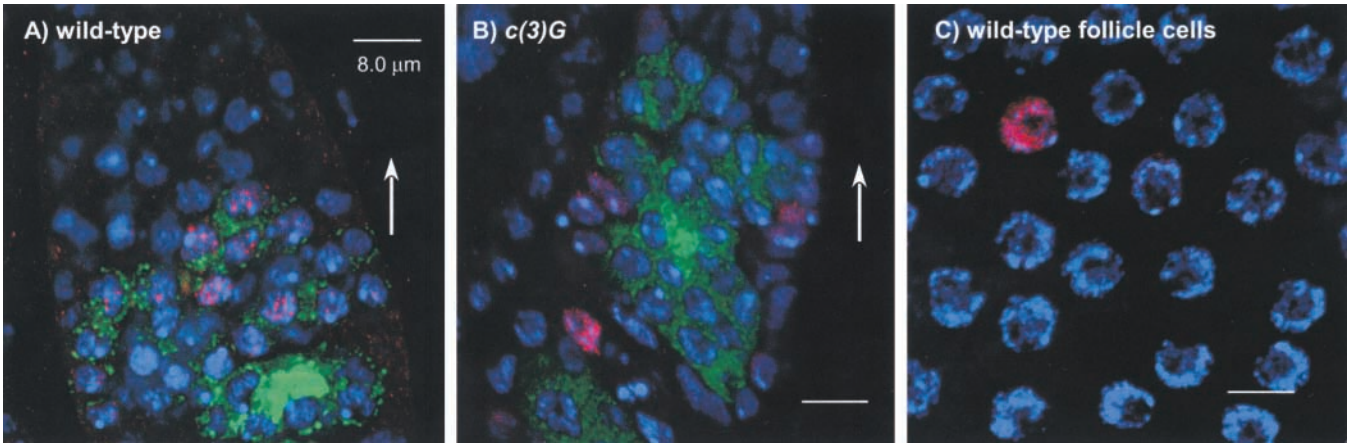

FIGURE 5.—MEI-P22 is localized to the nuclei of wild type but not of *c(3)G* mutants. (A) Wild-type germarium with MEI-P22 (red) appearing in the nuclei (DNA in blue) of the earliest cyst in region 2a with cytoplasmic ORB (green) staining. (B) MEI-P22 is absent in *c(3)G* mutant oocytes. Volume projection of a *c(3)G* mutant germarium with ORB to show these are region 2a cysts where MEI-P22 would normally be. The few nuclei with red staining are follicle cells. In A and B, an arrow indicates the anterior end of the germarium. (C) MEI-P22 in the mitotically dividing somatic follicle cells. The focal plane of this image is the outside edge of an ovarian stage 3 cyst. This cyst is located in the vitellarium, the region after the germarium. BrdU incorporation experiments showed that this expression pattern did not correspond to S-phase (data not shown). Within the nucleus of these cells, MEI-P22 colocalizes with the DNA and has a fibrous appearance, suggesting that it is binding to the chromosomes, although there are no discrete foci. Bars, 8 μm.

with C(3)G in these mutants, there were more cysts per germarium with MEI-P22 foci in the two pro-oocytes. In wild type, approximately four cysts with MEI-P22 staining were in the pro-oocytes, whereas in these mutants approximately six cysts with MEI-P22 staining were in the two pro-oocytes (Table 3). Both mutants and wild type had a similar number of cysts in each germaria and the increase in the mutant germaria could be attributed to an increased number of consecutive cysts with pro-oocyte MEI-P22 staining. One explanation for these results is that DSB repair may increase the rate at which MEI-P22 is removed from the chromosomes. Even in the absence of DSB repair, however, MEI-P22 foci were not observed later in prophase (region 3). Therefore, other factors must have a role in regulating MEI-P22 chromosome binding.

If DSB repair increases the rate at which MEI-P22 is removed from chromosomes, the relatively high abundance of MEI-P22 foci in pro-nurse cells can be explained. In the cells that never complete SC formation (pro-nurse cells), the rate of DSB repair may be lower than that in the cells where SC forms completely (pro-oocytes). The low rate of DSB repair in the pro-nurse cells could occur because they only partially enter the meiotic program. Consistent with this hypothesis, in the mutants without DSB repair the MEI-P22 foci appeared and then disappeared with similar dynamics in both the pro-oocytes and the pro-nurse cells.

The frequency of MEI-P22 foci: We counted the number of MEI-P22 foci in nuclei with the strongest C(3)G staining, the two cells with four ring canals. We focused on these cells for two reasons: first, they are the only cells in each cyst that reliably achieve full synapsis of the homologs (pachytene) and second, one of these cells will become the oocyte for which genetic data on recombination frequencies are available for comparison. In wild type, we counted an average of 8.7 foci per cell whereas, on the basis of limited data, we estimate ~15 per DSB per nucleus [on the basis of the estimate of one crossover every five gene conversions at the *rosy* locus (HILLIKER and CHOVNICK 1981) that the crossing over at the *rosy* locus is less frequent (~1/2) than the genome average and that there is an average of 1.2 crossovers per chromosome arm]. It is likely that the lower number of MEI-P22 foci was due to their dynamic and transient nature in the pro-oocytes.

MEI-P22 localization on the chromosomes is *c(3)G* dependent: In *c(3)G* mutants, SC does not develop (SMITH and KING 1968; RASMUSSEN 1975) and meiotic recombination is drastically reduced (CARLSON 1972; HALL 1972). To investigate the possibility that C(3)G is required to recruit proteins required for DSB formation to meiotic chromosomes, we constructed *hsp83::mei-P22^{3XHA}; c(3)G^{68}* females. In these females, we did not detect MEI-P22 foci in the germline (Figure 5B, $n = 13$), providing a strong correlation between the presence of the foci and meiotic recombination. It is possible that MEI-P22 stability or localization to meiotic chromosomes requires the SC.

DISCUSSION

What do the MEI-P22 foci represent? Several lines of evidence support the conclusion that *mei-P22* is required

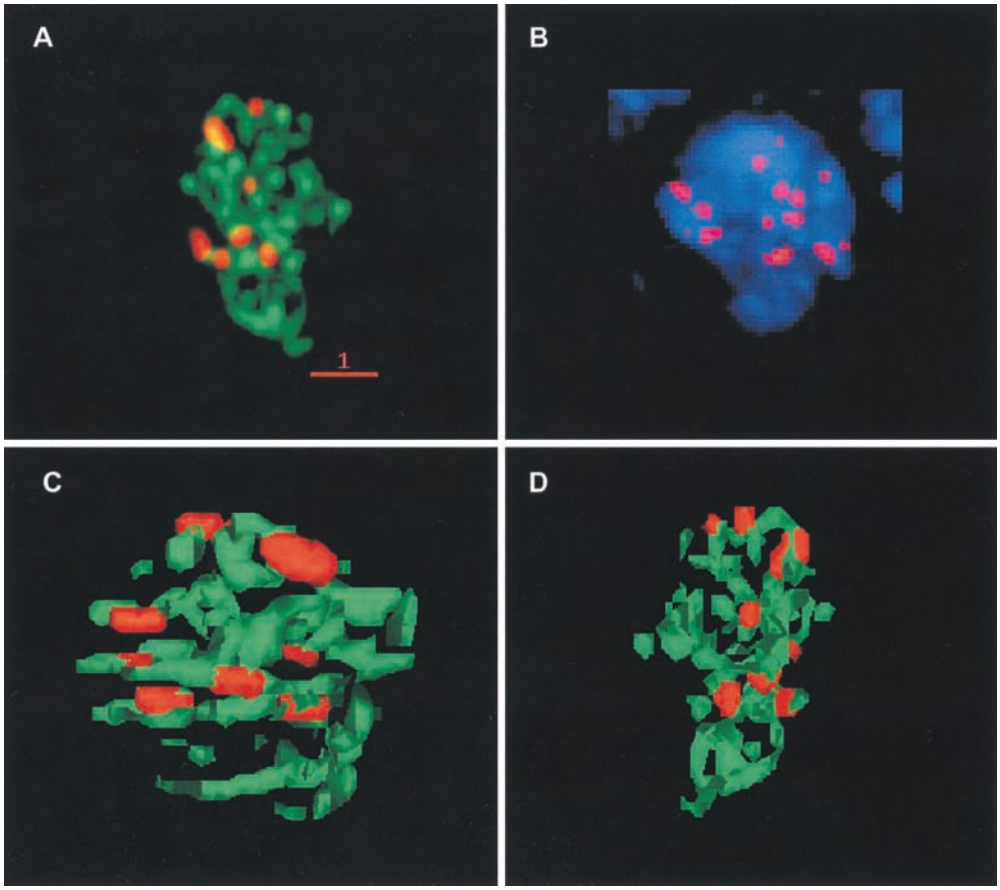

FIGURE 6.—MEI-P22 is nuclear and co-localizes with the DNA but not C(3)G. (A) Image following deconvolution and projection of the stack with MEI-P22 (red) and C(3)G (green). The frequent presence of red and infrequent presence of yellow staining indicate that most of the MEI-P22 staining does not overlap with C(3)G. Bar, 1 μm. (B) A similar type of image from a different nucleus showing MEI-P22 (red) is always associated with the DNA (blue). (C and D) A model of the nucleus shown in A with the two images rotated 90° relative to each other to show that the MEI-P22 foci are adjacent to the SC. As is typical for wild type, 10 foci are visible (see text).

for an early step in recombination during Drosophila meiosis. First, both gene conversion and crossing over are eliminated in strong *mei-P22* mutants (McKIM *et al.* 1998 and this article). Second, *mei-P22* mutants suppress the sterility phenotype of DSB repair-defective mutants such as $spnB^{BU}$. Third, crossing over is restored by an exogenous source of double-strand breaks, implying that *mei-P22* mutants lack them. Finally, the staining by an antibody that detects histone modifications at DSB sites, γ-H2AX, is eliminated in *mei-P22* mutants. From the similarity of these phenotypes to those observed in *mei-W68* mutants, we hypothesize that *mei-P22* is required for DSB formation.

Our most significant and novel finding is that MEI-P22 is found as chromosome-associated foci early in meiotic prophase. In our results, the strong correlation between the presence of MEI-P22 foci and meiotic recombination suggests that these foci are relevant to DSB formation. The MEI-P22 foci are present at a narrower window of time during pachytene than is the pattern of RNA expression, making it likely that the appearance and disappearance of the foci are unrelated to the promoter used and instead are a product of post-transcriptional regulation. During this portion of pachytene, the early recombination nodules appear on the chromosomes (CARPENTER 1975b). Early recombination nodules are the structures proposed to be associated with early stages of meiotic recombination and are observed at the same time, early pachytene (region 2a of the germarium), as the MEI-P22 foci are observed. This correlation suggests that there may be a relationship between the MEI-P22 foci and DSB formation.

Several additional observations support a functional significance between the MEI-P22 foci and DSB sites. For instance, the MEI-P22 foci are influenced by mutations in other meiotic recombination genes. The MEI-P22 foci are absent in a *c(3)G* mutant in which the SC does not form, and they persist in the oocyte for a longer time in mutants that do not induce or repair DSBs. Also, MEI-P22 foci form only in the germline and their numbers are similar to the predicted number of recombination events in the genome. Finally, there was a perfect correlation between the transgenes that rescued the *mei-P22* mutant phenotype and the presence of the foci. In combination with the genetic results summarized above, and on the basis of these cytological observations, we suggest that the MEI-P22 foci represent the sites along the chromosomes where DSBs will form.

Similar examples in other systems of proteins required for DSB formation to be found localized to meiotic chromosomes are limited. In *S. cerevisiae*, the Mre11/Rad50/Xrs2 complex has been observed, but is

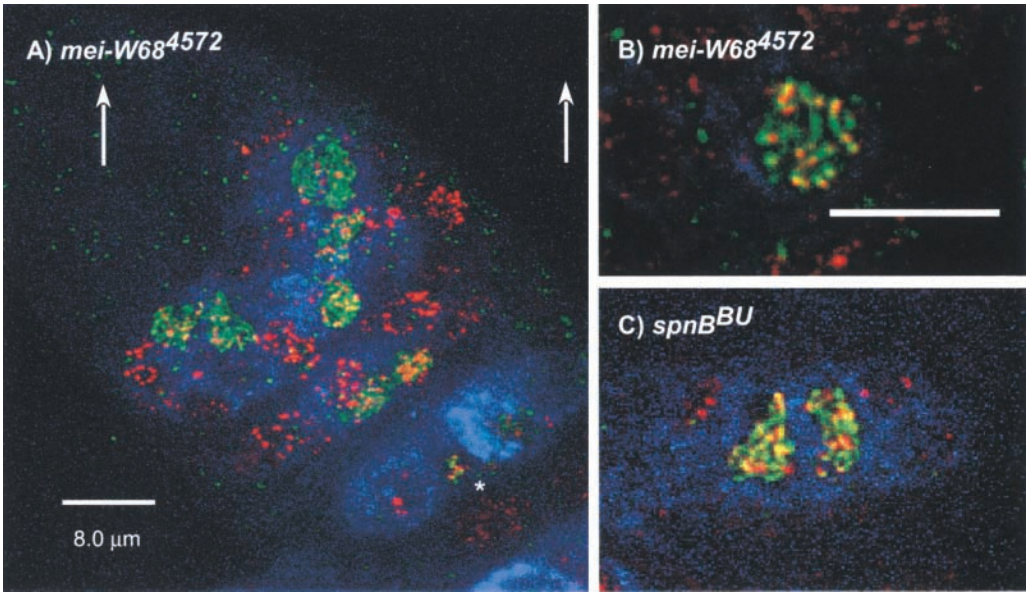

FIGURE 7.—Expression of MEI-P22 (shown in red) in meiotic mutants. MEI-P22 is present in *mei-W68* (A and B) and *spnB* (C) mutants. (A) A volume projection of a germarium showing normal appearance of MEI-P22 (red) in region 2a along with C(3)G (green) and ORB (blue) but unusual persistence into region 2b (indicated by an asterisk). (B and C) Single confocal sections showing that MEI-P22 is associated with the C(3)G of region 2b cysts.

visible only in a *rad50S* mutant where DSBs accumulate because they are not resected and repaired (USUI *et al.* 1998). This complex was also observed in male mouse meiosis but there was no correlation with DSB sites (EIJPE *et al.* 2000). More relevant to our findings is the Rec102 protein. This *S. cerevisiae* meiosis-specific protein is required for DSB formation and has been observed as foci on meiotic chromosomes by immunofluorescence (KEE and KEENEY 2002).

MEI-P22 foci and DSB formation are dependent on chromosome structure: If we assume that MEI-P22 foci respond to the same factors that regulate meiotic recombination, our observations provide a view of the regulatory mechanisms that ensure that only a small number of DSBs are generated in each cell. We propose the following sequence of events for regulating MEI-P22 and DSB formation in Drosophila female meiosis (Figure 4A). First, the homologs align and form SC. Second, SC-dependent changes in chromatin structure provide the conditions that promote MEI-P22 accumulation at discrete chromosome sites. If MEI-P22 is not expressed early enough, it may not be able to gain access to the chromosomes. Third, MEI-P22, and likely other proteins, promote the DSB activity of the Spo11 homolog MEI-W68. The observation that MEI-P22 foci are observed in the absence of DSB activity (*i.e.*, a *mei-W68* mutant) demonstrates that MEI-P22 is not recruited to chromosomes in response to a breakage event. Finally, the MEI-P22 foci begin to disappear, first from the pachytene cells and later from the other cells that form partial SC.

The dependence of MEI-P22 localization on C(3)G is consistent with genetic studies in Drosophila females where meiotic recombination does not occur in the absence of SC (CARLSON 1972; HALL 1972; PAGE and HAWLEY 2001) and SC can form normally between homologs in the absence of recombination (MCKIM *et al.* 1998). C(3)G and SC formation are not sufficient, however, for MEI-P22 localization. In later stages of pachytene, regions 2b and 3, C(3)G is still assembled between the homologs but MEI-P22 foci are never present. The disappearance of MEI-P22 is not due to transcriptional regulation and demonstrates that the SC has an essential but not sufficient role in regulating MEI-P22 accumulation. In fact, the completion of synapsis may have a negative influence on the foci (see below).

Limiting the time when MEI-P22 binds to chromosomes may regulate DSB formation: The brief appearance of MEI-P22 in region 2a cells demonstrates that its expression is tightly controlled. Our evidence suggests that the rapid removal of MEI-P22 foci may be related to DSB repair activities, which for a number of reasons could be more efficient in the oocyte. For example, complete SC formation might stimulate DSB repair. Alternatively, and akin to SC formation in the 16-cell cyst, DSB repair proteins might be present in the greatest concentration in the two prospective oocytes. The ultimate inhibition or removal of MEI-P22 foci, however, occurs even in the absence of DSBs and therefore is unrelated to DSB repair. Our observations are consistent with two nonexclusive processes that may have a role in the final removal and/or inhibition of MEI-P22 chromosome binding. First, the nuclear localization and chromosome binding of MEI-P22 in the germline may be regulated by a mechanism involving cell-cycle controls that also function in mitotic cells. This has an obvious evolutionary attraction, given that meiosis is thought to have evolved from a mitotic cell cycle. Second, not only is the SC required for the formation of MEI-P22 foci but also its maturation and/or complete synapsis may contribute to their disappearance. This inhibition of foci formation may correspond

to changes in SC morphology previously noted by Carpenter (1975a). As the cells reach pachytene, the SC progressively shortens and thickens. The corresponding structural changes to the SC could modify the chromosomes such that MEI-P22 can no longer bind and therefore prevent further DSB formation.

There are two reasons to regulate DSB formation within the cell. First, the timing of DSB formation is important for its meiotic function. The analysis of X-ray-induced crossing over shows that for DSBs to effectively induce crossovers, they must occur during pachytene. Second, once a sufficient number of DSBs have been induced, the activity of generating breaks must then be attenuated. Failure to stop the induction of breaks could lead to excessive chromosomal breakage and cell lethality. It is reasonable to conclude from the foci dynamics that MEI-P22 is under the control of a system regulating DSB formation. The ability to directly observe MEI-P22 localizing to potential DSB sites will facilitate further studies on the mechanisms that regulate DSB formation.

We are grateful to Rajal Bhagat and Dalia Sherizen for help with the screen for *mei-P22* alleles; to Hugo Dooner, R. Scott Hawley, Ken Irvine, Elizabeth Manheim, Ruth Steward, and Anne Villeneuve for insightful discussions and comments on the manuscript; to Eric Lam in whose laboratory the deconvolution microscopy was performed; to Jay Tischfield for use of an X-irradiator; to Brian Calvi and Mary Lilly for advice on BrdU labeling; and to Li Nguyen for technical assistance. We also thank Scott Page and Scott Hawley for providing the C(3)G antibody and data prior to publication. The initial molecular characterization and sequencing of the *mei-P22* locus was carried out in the laboratory of R. Scott Hawley. Some of the stocks used in this study were received from the Bloomington Stock Center. The ORB antibodies were obtained from the Developmental Studies Hybridoma Bank at the University of Iowa, developed under the auspices of the National Institute of Child Health and Human Development. This work was supported by grant MCB-0077705 from the National Science Foundation.

LITERATURE CITED

Ashburner, M., 1989 *Drosophila: A Laboratory Handbook*. Cold Spring Harbor Laboratory Press, Cold Spring Harbor, NY.

Baker, B. S., and J. C. Hall, 1976 Meiotic mutants: genetic control of meiotic recombination and chromosome segregation, pp. 351–434 in *The Genetics and Biology of Drosophila*, edited by M. Ashburner and E. Novitski. Academic Press, New York.

Belmont, A. S., M. B. Braunfeld, J. W. Sedat and D. A. Agard, 1989 Large-scale chromatin structural domains within mitotic and interphase chromosomes in vivo and in vitro. Chromosoma **98:** 129–143.

Carlson, P. S., 1972 The effects of inversions and the *c(3)G* mutation on intragenic recombination in Drosophila. Genet. Res. **19:** 129–132.

Carpenter, A. T. C., 1975a Electron microscopy of meiosis in *Drosophila melanogaster* females. I. Structure, arrangement, and temporal change of the synaptonemal complex in wild-type. Chromosoma **51:** 157–182.

Carpenter, A. T. C., 1975b Electron microscopy of meiosis in *Drosophila melanogaster* females. II. The recombination nodule—A recombination-associated structure at pachytene? Proc. Natl. Acad. Sci. USA **72:** 3186–3189.

Carpenter, A. T. C., 1979 Synaptonemal complex and recombination nodules in wild-type *Drosophila melanogaster* females. Genetics **92:** 511–541.

Carpenter, A. T. C., 1994 *egalitarian* and the choice of cell fates in *Drosophila melanogaster* oogenesis. Ciba Found. Symp. **182:** 223–254.

Celerin, M., S. T. Merino, J. E. Stone, A. M. Menzie and M. E. Zolan, 2000 Multiple roles of Spo11 in meiotic chromosome behavior. EMBO J. **19:** 2739–2750.

Dernburg, A. F., K. McDonald, G. Moulder, R. Barstead, M. Dresser *et al.*, 1998 Meiotic recombination in *C. elegans* initiates by a conserved mechanism and is dispensable for homologous chromosome synapsis. Cell **94:** 387–398.

Ding, D., S. M. Parkhurst, S. R. Halsell and H. D. Lipshitz, 1993 Dynamic *Hsp83* RNA localization during *Drosophila* oogenesis and embryogenesis. Mol. Cell. Biol. **13:** 3773–3781.

Eijpe, M., H. Offenberg, W. Goedecke and C. Heyting, 2000 Localisation of RAD50 and MRE11 in spermatocyte nuclei of mouse and rat. Chromosoma **109:** 123–132.

Finelli, A. L., C. A. Bossie, T. Xie and R. W. Padgett, 1994 Mutational analysis of the Drosophila *tolloid* gene, a human BMP-1 homolog. Development **120:** 861–870.

Ghabrial, A., and T. Schupbach, 1999 Activation of a meiotic checkpoint regulates translation of Gurken during Drosophila oogenesis. Nat. Cell Biol. **1:** 354–357.

Ghabrial, A., R. P. Ray and T. Schupbach, 1998 *okra* and *spindle-B* encode components of the RAD52 DNA repair pathway and affect meiosis and patterning in Drosophila oogenesis. Genes Dev. **12:** 2711–2723.

Goldman, A. S. H., and M. Lichten, 1996 The efficiency of meiotic recombination between dispersed sequences in *Saccharomyces cerevisiae* depends upon their chromosomal location. Genetics **144:** 43–55.

Hall, J. C., 1972 Chromosome segregation influenced by two alleles of the meiotic mutant *c(3)G* in *Drosophila melanogaster*. Genetics **71:** 367–400.

Hilliker, A. J., and A. Chovnick, 1981 Further observations on intragenic recombination in *Drosophila melanogaster*. Genet. Res. **38:** 281–296.

Kee, K., and S. Keeney, 2002 Functional interactions between *SPO11* and *REC102* during initiation of meiotic recombination in *Saccharomyces cerevisiae*. Genetics **160:** 111–122.

King, R. C., 1970 *Ovarian Development in Drosophila melanogaster*. Academic Press, New York.

Lantz, V., J. S. Chang, J. I. Horabin, D. Bopp and P. Schedl, 1994 The Drosophila ORB RNA-binding protein is required for the formation of the egg chamber and establishment of polarity. Genes Dev. **8:** 598–613.

Lichten, M., 2001 Meiotic recombination: breaking the genome to save it. Curr. Biol. **11:** R253–R256.

Mahadevaiah, S. K., J. M. Turner, F. Baudat, E. P. Rogakou, P. de Boer *et al.*, 2001 Recombinational DNA double-strand breaks in mice precede synapsis. Nat. Genet. **27:** 271–276.

Manheim, E. A., J. K. Jang, D. Dominic and K. S. McKim, 2002 Cytoplasmic localization and evolutionary conservation of MEI-218, a protein required for meiotic crossing over in Drosophila. Mol. Biol. Cell **13:** 84–95.

McKim, K. S., B. L. Green-Marroquin, J. J. Sekelsky, G. Chin, C. Steinberg *et al.*, 1998 Meiotic synapsis in the absence of recombination. Science **279:** 876–878.

Myers, E. W., G. G. Sutton, A. L. Delcher, I. M. Dew, D. P. Fasulo *et al.*, 2000 A whole-genome assembly of Drosophila. Science **287:** 2196–2204.

Page, S. L., and R. S. Hawley, 2001 *c(3)G* encodes a *Drosophila* synaptonemal complex protein. Genes Dev. **15:** 3130–3143.

Rasmussen, S. W., 1975 Ultrastructural studies of meiosis in males and females of the *c(3)G* mutant in *Drosophila melanogaster* meigen. C.R. Trac. Lab. Carlsberg **40:** 163–173.

Roberts, P. A., 1969 Some components of X-ray-induced crossing over in females of *Drosophila melanogaster*. Genetics **63:** 387–404.

Roeder, G. S., 1997 Meiotic chromosomes: it takes two to tango. Genes Dev. **11:** 2600–2621.

Rogakou, E. P., C. Boon, C. Redon and W. M. Bonner, 1999 Megabase chromatin domains involved in DNA double-strand breaks in vivo. J. Cell Biol. **146:** 905–916.

Schwacha, A., and N. Kleckner, 1995 Identification of double Holliday junctions as intermediates in meiotic recombination. Cell **83:** 783–791.

Sekelsky, J. J., K. S. McKim, L. Messina, R. L. French, W. D. Hurley *et al.*, 1999 Identification of novel Drosophila meiotic genes recovered in a *P*-element screen. Genetics **152:** 529–542.

Smith, P. A., and R. C. King, 1968 Genetic control of synaptinemal complexes in *Drosophila melanogaster*. Genetics **60:** 335–351.

Spradling, A. C., M. de Cuevas, D. Drummond-Barbosa, L. Keyes, M. Lilly *et al.*, 1997 The Drosophila germarium: stem cells, germ line cysts, and oocytes. Cold Spring Harbor Symp. Quant. Biol. **62:** 25–34.

Szostak, J. W., T. L. Orr-Weaver, R. J. Rothstein and F. W. Stahl, 1983 The double-strand-break repair model for recombination. Cell **33:** 25–35.

Tautz, D., and C. Pfeifle, 1989 A non-radioactive in situ hybridization method for the localization of specific RNAs in *Drosophila* embryos reveals translational control of the segmentation gene *hunchback*. Chromosoma **98:** 81–85.

Thorne, L. W., and B. Byers, 1993 Stage-specific effects of X irradiation on yeast meiosis. Genetics **134:** 29–42.

Usui, T., T. Ohta, H. Oshiumi, J. Tomizawa, H. Ogawa *et al.*, 1998 Complex formation and functional versatility of Mre11 of budding yeast in recombination. Cell **95:** 705–716.

Communicating editor: S. Henikoff